P H Y S I C A L   R E V I E W   L E T T E R S

Self-Assembled Chiral Superstructures Composed of Rigid Achiral Molecules and Molecular Scale Chiral Induction by Dopants

Fangyong Yan, Christopher Adam Hixson, and David J. Earl[*]

Department of Chemistry and Center for Molecular and Materials Simulations, University of Pittsburgh, 219 Parkman Avenue, Pittsburgh, Pennsylvania 15260, USA

We explore the phase behavior of a rigid achiral bent-core model system. Nematic and smectic phases form at higher densities, whereas micelles and columns composed of chiral clusters of these molecules self-assemble at lower densities. No nucleation mechanism requiring transient chirality is possible in the formation of these chiral superstructures due to the rigid achiral nature of the substituents. We show the chiral micelles are minima of the potential energy surface using energy minimization and parallel tempering simulations. Chiral dopants were found to induce the system to adopt a consistent chiral twist direction, the first molecular scale computer simulation of this effect.

Macromolecular and nanoscale systems exhibiting superstructural chirality abound. In biological contexts, chiral helices can be found in DNA and proteins; twisted beta sheets form helical columns [1], as in silk, and modern synthetic analogues have appeared [2,3]. In materials science, examples include liquid crystalline cholesteric phases [4] and chiral smectic phases [5] formed from bent-core molecules. These systems each exhibit chirality that goes beyond an individual unit and extends into a superstructure or over an entire phase. Generally, the chirality is derived from the individual molecular components. Surprisingly, chirality can also arise spontaneously in systems that are composed of achiral molecules, for example, in the liquid crystalline banana phases [5,6], and in chiral crystals formed from ammonium salts and fatty acids [7]. Similarly, stable chiral structures can be formed from achiral particles due to templating [8] and stirring [9].

Chiral superassemblies are most commonly modeled by including explicit terms in intermolecular potential energy functions that favor the formation of chiral superstructures. For example, Memmer *et al.* found that chiral Gay-Berne particles form helices [10], whereas achiral Gay-Berne particles do not [11], Grason and Bruinsma [12] modeled biopolymer bundle aggregates by adding a twisting term to a free-energy expression, and Tepper and Voth [13] reproduced the DNA double twist using a model that incorporated frustration that was best satisfied in the double helix structure. Twisted structures have also been found in systems where interactions are not explicitly chiral. Fejer and Wales [14] cataloged the lowest potential energy structures of clusters of discotic Gay-Berne-like particles and found helical structures, Chakrabarti and Wales [15] recently demonstrated the formation of helical columnar phases using particles which interact via a Gay-Berne variant [16], and Horsch *et al.* predicted a hexagonal chiral cylinder phase in a system composed of flexible achiral polymer-tethered nanorods [17,18]. Although chiral

phases have been observed experimentally in bent-core systems [5] and previous theoretical and computational studies of these systems have revealed a variety of liquid crystalline phases [19–23], no previous theoretical models evince chirality.

In this Letter we explore the phase behavior of a coarse-grained bent-core model system using computer simulations, where the constituent molecules in our simulations are rigid and achiral. We have chosen to work with a simplified coarse-grained model system in order to determine the essential physics required to observe the chiral phenomena of interest here. We construct a phase diagram by characterizing the structures observed in molecular dynamics simulations at a range of temperatures and volume fractions. We present two major results. First, chiral superstructures can self-assemble from the rigid achiral molecules we study, although on the scale of the whole system we observe equal numbers of left- and right-handed structures. In order to understand the thermodynamic basis for the stability of these structures, we performed Monte Carlo parallel tempering simulations and energy minimization calculations on small clusters of these molecules. Second, we demonstrate control of the supramolecular chirality by the addition of low concentrations of chiral dopants. We find that the dopants can induce a consistent twist sense over the entire phase, the first molecular scale simulation of this effect.

The details of our model are as follows: each rigid molecule is composed of N beads, each of mass m. A subset containing N_A beads interacts using an intermolecular Lennard-Jones (LJ) potential. The remaining $N_B = N - N_A$ beads interact using an intermolecular Weeks-Chandler-Andersen (WCA) potential [24]. Intermolecular A-B interactions use a WCA potential. Each subset of beads is arranged in a linear segment, with each particle separated by length σ. The two linear segments are joined together into a single rigid molecule with an angle of γ between the two segments (see Fig. 1). In this Letter, we
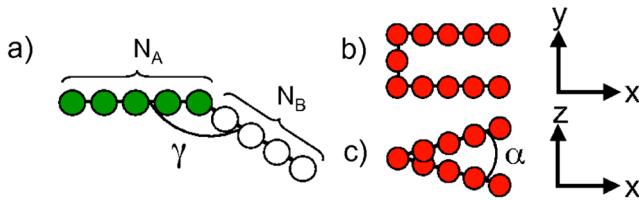
FIG. 1 (color online).   Two model molecules were employed in this work. (a) The bent-core model, composed of LJ [shaded (green)] and WCA (white) particles, with the fixed angle, γ, defining the rigid, achiral shape of the molecule. We found that the twist direction of the structures formed by the bent-core molecules could be controlled by adding chiral dopants, composed of LJ [dark shaded (red)] particles. The chiral dopant molecule is shown in the (b) xy plane and the (c) xz plane. The angle, α, defines the twist sense of the dopant molecule.

FIG. 2 (color online).   Phase diagram of the bent-core system. $T^* = k_B T/\epsilon$ is the reduced temperature and $\phi = MN\pi\sigma^3/V_{\text{box}}$ is the volume fraction. At volume fractions greater than 0.21, the system visits the nematic (N), lamellar (L), smectic A (SmA), smectic C (SmC), and smectic I (SmI) phases. At lower densities, chiral features develop, including chiral micelle (CM) and chiral column (CC) phases. We find the isotropic (Iso) phase at high temperatures for all volume fractions.

have chosen to work with a system of $M = 4800$ molecules, with $N_A = 5$, $N_B = 4$, and $\gamma = 150°$. The molecule may be interpreted as a rigid-shape amphiphile in a solvent that is good for the WCA section and poor for the LJ section. Simulation details and results are presented in terms of reduced units [25].

Our molecular dynamics simulations were performed using a pair potential cutoff of 2.5σ and a time step of $5 \times 10^{-3}t^*$. We integrated the equations of motion using the NO_SQUISH integrator of Miller *et al.* [26] and used an operator splitting similar to that proposed by Kamberaj *et al.* [27] for simulations in the canonical and isothermal-isobaric ensembles. The system was prepared at a variety of densities, and heated until the isotropic phase was observed in the *NVT* ensemble. The system was then sequentially cooled 0.25 reduced temperature units over 1.5×10^5 steps followed by an equilibration period of 3×10^5 steps. Near phase transitions this process was slowed and manually observed to ensure equilibrium was maintained. We also performed simulation runs in the isothermal-isobaric (*NPT*) ensemble, where systems were prepared in the isotropic phase at a variety of pressures and then slowly annealed following the same procedure as the *NVT* simulations. The phases we report in this Letter were observed in both our *NVT* and *NPT* simulations, and a phase diagram for the bent-core system is shown in Fig. 2. We construct our phase diagram in a manner similar to Horsch *et al.* [17,18].

At high volume fractions, the system visits a range of traditional liquid crystalline phases. A lamellar phase (L) exists at volume fractions beyond $\phi = 0.21$. This phase is characterized by layers formed by the Lennard-Jones portion of the model, separated by disordered layers of the purely repulsive WCA portion. We find regions of smectic ordering at volume fractions greater than 0.27 including smectic A, smectic C, and smectic I phases. The smectic I phase possesses local hexagonal ordering along with an in-layer tilt towards the hexagonal apex. The presence of attractive and replusive regions in our model naturally
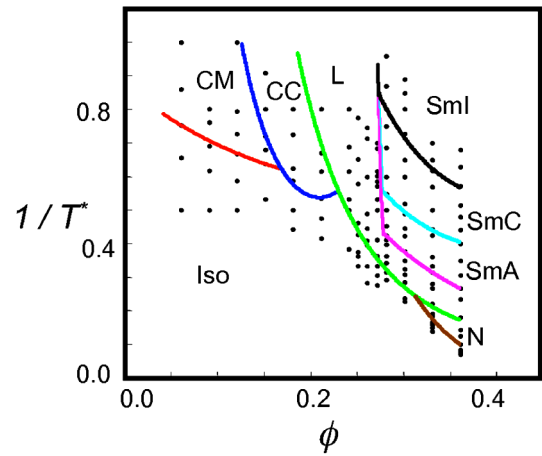
favors zigzag configurations of particles at high density. Thus, we believe that the origin of the in-layer tilt arises for steric reasons, as occurs in systems composed of purely repulsive zigzag shaped particles [28]. The tilt angle varies with temperature and pressure, and has a maximum of 27°. The large system size that we use ensures that we have at least three discrete smectic layers in the periodic simulation box. We also observe a nematic phase (N) at higher temperatures, for volume fractions between $\phi = 0.33$ and 0.36.

At volume fractions up to $\phi = 0.15$ on the phase diagram, a phase composed of chiral micelles (CM) forms. A snapshot of this phase is shown in Fig. 3(a). The micelles are stabilized due to the attractive LJ sections' tendency to adhere to each other, which is counterbalanced by the space-filling, purely repulsive nature of the WCA portions. This balance leads to a racemic polydisperse size distribution of micelles. The noteworthy nature of this result is found in the chiral nature of the micelles. There is a discernible twist in each, shown in Figs. 3(f) and 3(g), that is also observed in parallel tempering simulations and energy minimizations of small clusters of the model system.

To determine the thermodynamic basis for the stability of the chiral micelles, we explored the potential energy surfaces of clusters of 2, 4, 8, and 60 molecules, using energy minimization techniques and parallel tempering simulations. For clusters of 2, 4, and 8 molecules, our minimizations were performed using the basin hopping technique [29] with the Polak-Ribiere conjugate gradient method as the underlying minimization scheme [30]. Parallel tempering simulations [31] were performed for
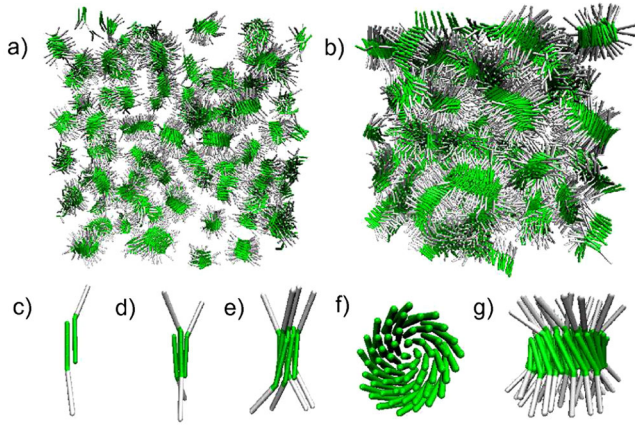
FIG. 3 (color online).   (a) Chiral micelle snapshot. (b) Chiral column snapshot. Energy minimized structures of (c) two, (d) four, and (e) eight molecule clusters of the model system. Minimization of the energy requires maximum overlap between attractive sites, which ultimately manifests as a structural twist. Parallel tempering simulations reproduce the observed twisted micelle shape which is shown (f) from a top down view with the WCA sections removed and (g) from the side.

systems containing 60 molecules, a typical size for a chiral micelle in our simulations, inside a spherical enclosure of radius 25σ. These simulations used Monte Carlo moves that changed the center of mass position and orientation of randomly selected molecules. Eighteen parallel tempering replicas were used, with a low temperature of $T^* = 0.6$ employed. The temperatures of other replicas were allowed to adaptively vary until the swapping ratios were optimized [32]. Low energy configurations from these simulations were stored and energy minimized. The minimizations indicate that the discrete nature of the interactions in the model cause twisting as a means to minimize the potential energy, demonstrated by the staggered alignment of molecules shown in Figs. 3(c)–3(g). This corresponds to off-center alignment in the two molecule system, a staggered square arrangement in the four molecule system, and the beginnings of a twisted barrel in the eight molecule system. The parallel tempering simulations found twisted barrel-shaped structures with both possible twist directions with nearly identical energies, which is consistent with our observed racemic mixture in the CM phase. Untwisted micelles were only observed in higher temperature replicas and had unfavorable energies compared to the twisted structures. In simulations of flexible polymer-tethered nanorods, Horsch et al. also observed ordered micelle phases [18,33]. In a laterally tethered system, the micelles formed by stacking into a staircase shape, which lacked twisting. In an end-tethered system, twisting barrel shapes were observed. Because of the similarity of the rigid LJ portion of our molecule to those in these studies, the thermodynamic argument explaining the stability of the twisted superstructures is expected to be the same in both cases.

A second chiral phase is noted in Fig. 2. This phase, described as a chiral column phase (CC), is located between $\phi = 0.12$ and 0.21 and is pictured in Fig. 3(b). A more detailed view of the interior of an individual column can be seen in Fig. 4. In this phase, the structures possess a helical twist about the long axis of each column, which is interrupted if columns with differing handedness merge. Within the columns, a barrel-like chiral twist is evident. Though we have explored the nature of the chirality of the isolated micelles, explaining the helical twist observed in this phase is more complicated. Certainly, the packing of chiral objects together is likely to form a chiral structure, as would be the case for several micelles merging to form the column. However, the free energy of the double twist structure we observe is stabilized by the rotational entropy gained by an off-parallel stacking between all pairs of adjacent molecules, when compared with the achiral layered structures that are found at higher densities, although the twisted barrel-like structures within the columns are stabilized for the same energetic reasons as in the CM phase. We note that a helical twist was observed in the flexible-tether system of Horsch et al. [18] that was explained as an entropic effect, and a long ribbon phase was observed for laterally tethered rods [33].

To investigate whether the handedness of the chiral superstructures formed in the CM and CC phases could be controlled, we conducted molecular dynamics simulations at the densities at which these phases were found, where 1%, 2%, and 4% of the molecules in the system were replaced with chiral dopants. A schematic diagram showing the chiral dopant molecule used in the study is shown in Figs. 1(b) and 1(c). We used an angle of $\alpha = 15°$ between the two long axes of the dopant, corresponding to a right-hand twist sense for chiral dopants when added to nematic phases [34]. We found that if a dopant molecule was
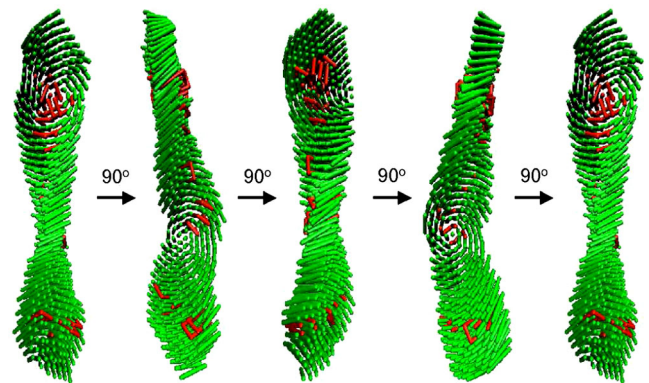

FIG. 4 (color online).   Rotated views of a single chiral column structure with dopant molecules [shown in dark shade (red)] incorporated. The WCA particles in the bent-core molecules have been removed to show the underlying structure of the column. As the dopants strongly influence the twist of the individual micelles into which they incorporate, the uniformity of the twist direction can be described as a packing effect.

incorporated into an individual micelle barrel then, due to packing effects, the handedness of the barrel's twist matched that of the chiral dopant. This result holds for all cases where a dopant molecule is incorporated into the structure. We found that the addition of as little as 4% dopant can cause the entire system to exhibit a uniform handedness. For doped chiral column systems the helical twist along the long axis of a column is completely uninterrupted, and the structure has a continuous double twist motif. Shown in Fig. 4 is an example of a doped column where the underlying twist sense within, and about, the column is right handed.

That chiral structures can be found in a material composed of rigid achiral building blocks is of further interest because it rules out any nucleation mechanism requiring transient chirality [7,35]. In systems composed of flexible achiral molecules, although the constituent molecules are achiral on average, each molecule can instantaneously adopt a chiral configuration, and one may argue that the clustering of molecules with the same handedness results in the formation of chiral structures (although there would be an overall racemic mixture of chiral structures). In our study, then, no such mechanism is possible as our constituent molecules are fixed in an achiral conformation. Thus, our results may have implications for the underlying physics behind the formation of some of the liquid crystal banana phases [5], for the stability of blue phases when doped with banana molecules [36], and for the design and synthesis of chiral fibers [37] and crystals [7].

*dearl@pitt.edu; http://www.pitt.edu/~dearl

[1] C. Chothia, J. Mol. Biol. **75**, 295 (1973).

[2] T. Muraoka, H. Cui, and S. I. Stupp, J. Am. Chem. Soc. **130**, 2946 (2008).

[3] L. Li, H. Jiang, B. W. Messmore, S. R. Bull, and S. I. Stupp, Angew. Chem., Int. Ed. **46**, 5873 (2007).

[4] P. G. de Gennes, *Physics of Liquid Crystals* (Oxford Univeristy, New York, 1993).

[5] R. A. Reddy and C. Tschierske, J. Mater. Chem. **16**, 907 (2006).

[6] D. R. Link, G. Natale, R. Shao, J. E. Maclennan, N. A. Clark, E. Korblova, and D. M. Walba, Science **278**, 1924 (1997).

[7] A. Tanaka, K. Inoue, I. Hisaki, N. Tohnai, M. Miyata, and A. Matsumoto, Angew. Chem., Int. Ed. **45**, 4142 (2006).

[8] E. D. Sone, E. R. Zubarev, and S. I. Stupp, Angew. Chem., Int. Ed. **41**, 1705 (2002).

[9] J. M. Ribo, J. Crusats, F. Sagues, J. Claret, and R. Rubires, Science **292**, 2063 (2001).

[10] R. Memmer, H.-G. Kuball, and A. Schonhofer, Liq. Cryst. **15**, 345 (1993).

[11] P. Mishra, J. Ram, and Y. Singh, J. Phys. Condens. Matter **16**, 1695 (2004).

[12] G. M. Grason and R. F. Bruinsma, Phys. Rev. Lett. **99**, 098101 (2007).

[13] H. L. Tepper and G. A. Voth, J. Chem. Phys. **122**, 124906 (2005).

[14] S. N. Fejer and D. J. Wales, Phys. Rev. Lett. **99**, 086106 (2007).

[15] D. Chakrabarti and D. J. Wales, Phys. Rev. Lett. **100**, 127801 (2008).

[16] M. A. Bates and G. R. Luckhurst, J. Chem. Phys. **104**, 6696 (1996).

[17] M. A. Horsch, Z. Zhang, and S. C. Glotzer, Phys. Rev. Lett. **95**, 056105 (2005).

[18] M. A. Horsch, Z. Zhang, and S. C. Glotzer, J. Chem. Phys. **125**, 184903 (2006).

[19] R. Memmer, Liq. Cryst. **29**, 483 (2002).

[20] R. Hashim, G. R. Luckhurst, and S. Romano, J. Chem. Soc., Faraday Trans. **91**, 2141 (1995).

[21] Y. Lansac, P. K. Maiti, N. A. Clark, and M. A. Glaser, Phys. Rev. E **67**, 011703 (2003).

[22] A. Dewar and P. J. Camp, Phys. Rev. E **70**, 011704 (2004).

[23] S. Orlandi, R. Berardi, J. Steltzer, and C. Zannoni, J. Chem. Phys. **124**, 124907 (2006).

[24] J. D. Weeks, D. Chandler, and H. C. Andersen, J. Chem. Phys. **54**, 5237 (1971).

[25] M. P. Allen and D. J. Tildesley, *Computer Simulations of Liquids* (Oxford University, Oxford, 1989), pp. 327–328.

[26] T. F. Miller, III, M. Eleftheriou, P. Pattnaik, A. Ndirango, N. D., and G. J. Martyna, J. Chem. Phys. **116**, 8649 (2002).

[27] H. Kamberaj, R. J. Low, and M. P. Neal, J. Chem. Phys. **122**, 224114 (2005).

[28] P. K. Maiti, Y. Lansac, M. A. Glaser, and N. A. Clark, Phys. Rev. Lett. **92**, 025501 (2004).

[29] D. J. Wales and H. A. Scheraga, Science **285**, 1368 (1999).

[30] W. H. Press, S. A. Teukolsky, W. T. Vetterling, and B. P. Flannery, *Numerical Recipes* (Cambridge University Press, Cambridge, England, 2007).

[31] D. J. Earl and M. W. Deem, Phys. Chem. Chem. Phys. **7**, 3910 (2005).

[32] A. Kone and D. A. Kofke, J. Chem. Phys. **122**, 206101 (2005).

[33] M. A. Horsch, Z. Zhang, and S. C. Glotzer, Nano Lett. **6**, 2406 (2006).

[34] D. J. Earl and M. R. Wilson, J. Chem. Phys. **119**, 10 280 (2003).

[35] D. J. Earl, M. A. Osipov, H. Takezoe, Y. Takanishi, and M. R. Wilson, Phys. Rev. E **71**, 021706 (2005).

[36] H. J. Coles and M. N. Pivnenko, Nature (London) **436**, 997 (2005).

[37] A. Brizard, R. Oda, and I. Huc, in *Low Molecular Mass Gelators, Design, Self-Assembly, Function*, edited by F. Fages, Topics in Current Chemistry Vol. 256 (Springer, Berlin, 2005).